Ashish Bhave*, Stefan J. Rupitsch, Knut Moeller.

Analysis of stretch distribution of high compliant elastomers within folded lumen vessels

https://doi.org/10.1515/cdbme-2023-1172

Abstract: Elastomer based high compliant balloons containing strain sensing element(s) (SEs) is currently under development intended for in-vivo biomechanical diagnostics of vessels. It could potentially reveal local lumen features based on patterns derived from the sensing elements.

A Finite Element based, simulation study in COMSOL® (v5.6) focusses on in-vivo inflation behavior of an elastomeric balloon being equipped with SE, whose compliance is ideally magnitudes higher than the surrounding tissue in an idealized 2D setup. We hypothesized the vessel's inner wall as a closed convex-concave 4-fold structure correlated to surface structures found in urethrae and parameterized the fold depth. A set of SEs consisted of one SE over the inner surface of balloon while the other over the outer wall. Out of the three adjacent placed sets, The first set was closer to the tissue lumen while the third set the farthest.

We assessed the stretch of balloon over its inner circumference through SEs. At conformal contact with the tissue wall, The first SE shows a higher value, while the third element undergoes the least stretch within the three sensing elements. The SE's over the outer circumference show the exact opposite relation. The differences between the sensing elements over the inner and outer circumferences show a correlation with the curvature of the tissue it conforms to. With use of balloon that was 10x thicker (10µm vs 1µm), around 10x larger stretch differences were captured suggesting possibility to use less sensitive measuring system.

For the ideal situations performed, the curvature and depth information may be comprehended by observing differences between inner and outer SEs while thicker balloons prove to be more useful to generate differences that are easier to capture in practical situations. This semiquantitative study suggests that simulation studies are powerful tools to obtain new analytical techniques for shape characterization.

Keywords: Elastomers, Strain Sensing, Shape characterization, biomechanics, lumen.

1 Introduction

A high compliant inflatable intra-luminal sensor-actuator system is currently under development at the research institutes of Furtwangen University for application within urethra/artery [1].

In urethra, irregular shapes in the inner lumen are quite common [2] and in arteries, may be possible due to atherosclerosis and other pathologies [3]. Previous simulation studies have demonstrated that the local stretch of the tissue is influenced by the multifold/irregular shape of lumen inherent to vascular /urethral structures [4]. This may influence the outputs of identified tissue material properties based on general stretch evolution. To support this development, research was presented to show that the sensing elements (SE) embedded within the balloon provide local stretch information that is correlated to the lumen profile [5]. The stretch ratio between elements is influenced by the surrounding tissue shape.

In previous study for ideal cylindrical vessels, it was revealed that balloon thickness may not influence identification of tissue properties [6]. In situations that are non-cylindrical though, it becomes of importance to first understand the evolved stretches on the balloon parameterizing its thickness and later establish some analytical ratios focussed on vessel shape information and enable identification optimization techniques.

Corresponding author: Ashish Bhave: Institute of Technical Medicine, Furtwangen University, Jakob-Kienzle-Straße 17, Villingen-Schwenningen, Germany, e-mail: bha@hs-furtwangen.de
Stefan J. Rupitsch: Department of Microsystems Engineering, Georges-Köhler-Allee 106, Freiburg im Breisgau, Germany
Knut Moeller: Institute of Technical Medicine, Furtwangen University, Villingen-Schwenningen, Germany

2 Methods

It is important to understand the initial tissue geometry to determine local tissue properties and is attempted by using balloon stretch information using Sensing Elements (SE).

An aim of this study is to investigate the effect of balloon thickness on differences within the sensing elements placed on inner and outer circumference when expanded within multifold tissue geometries. The other aim is to analyse the differences within the SEs to obtain curvature and depth information.

Geometry initialization:

The balloon behavior is initialized by using Ogden model and parameter values as provided in [7] for material Sylgard® 184 (PolyDiMethylSiloxane- PDMS) and seen in Table 1. Figure 1.a shows the balloon with idealized embedded sensing elements that provide information about the circumferential strain. The circumference of the outer diameter of the balloon is initialized as $2 \times \pi$ mm ($\emptyset = 2$ mm) while its thickness is parameterized as 1µm and 10 µm respectively.

Table 1: Ogden 4 parameter model values.

Parameter	Value
α_1	2.17
α_2	9.06
α_3	34.3
α_4	-5.4
μ_1 [MPa]	2.91e-01
μ_2 [MPa]	3.40e-03
μ_3 [MPa]	2.01e-11
μ_4 [MPa]	1.15e-02
E [MPa]	1.09

The sensing elements (SE‘nr.’a) and (SE‘nr.’b) are placed on the inner and outer circumference of the balloon respectively and have a 1/16th length of its inner and outer circumference. Sensing elements (SE1a) is placed on the -90° (-y-axis) on the balloon’s inner circumference (blue in Fig. 1). The second (SE2a ; in green) and third (SE3a ; in red) sensing elements are placed adjacent to it in the anticlockwise direction, respectively. In the same manner the sensing elements ‘SE1b’ ‘SE2b’ and ‘SE3b’ are placed on the outer circumference shown in the blue, green and red regions respectively.

Figure 1b and 1c show a tissue with pure sinusoidal pattern of 4-folds, which are drawn along a circle. These structures ‘STR 1’ and ‘STR 2’ have sine wave amplitude of 0.2 mm, and 0.4 mm, respectively. The balloon lies

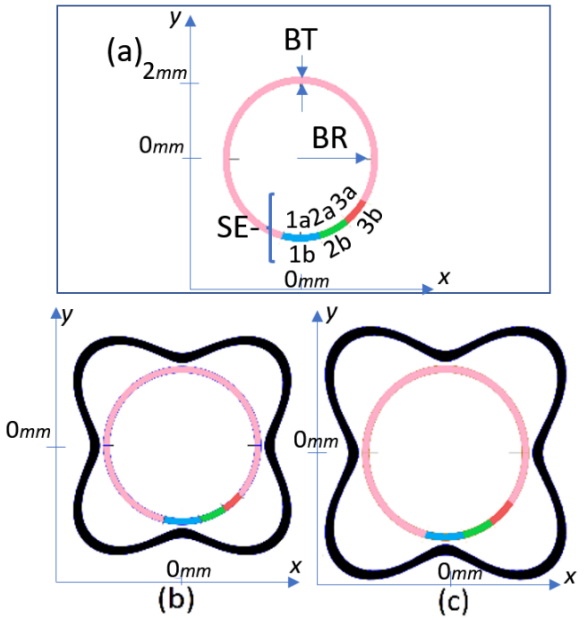

Figure 1: (a) depicts the 2d section of a balloon. Its thickness is parameterized as 1μm and 10μm. (b) shows balloon within Structure 1 having sinusoidal lumen profile (c) shows balloon within Structure 2 that is like Structure 1 but with the sinusoidal folds having twice the amplitude.

within these structures and the closest point of the tissue lumen is 0.1 mm from the balloon.

For evaluation and first insights into the problem, we chose a simple case where the structures are symmetric over the diagonals, the x- axis, and the y-axis. If more SEs were added adjacent to the above elements, each would have a mirrored stretch response to either one of the previously initialized elements. Therefore, more such elements were excluded for evaluation given the chosen ideal geometries of tissues.

The balloon and tissue are discretized into fine mapped mesh elements and the elements length on balloon to tissue ratio is greater than 2 to obtain numerically valid solutions.

Boundary Conditions:

Both the tissue models surround the balloon and have its external boundary as a fixed boundary condition. The tissue, therefore, may not deform during the balloon expansion and interaction with the tissues.

We applied standard boundary conditions like symmetry on the vertical and horizontal nodes of the structures that lie on the x- and y-axis for each simulation case. The inflation simulation is conducted as a time-dependent study with the pressure applied on the inner wall of the balloon. The applied pressure was increased from 0 kPa to 10 kPa in steps of 0.1 kPa. The used solver is allowed to choose a free time stepping over the range and

interpolate. The contact between the balloon and the stiff tissue structure is solved by the penalty method.

The circumferential stretch at the saturation level (the pressure at which the balloon has a complete conformal contact with the tissue) is recorded by each SE. To understand shape information for these ideal tissue shapes, we performed an analysis focused on the ratio of differences between stretch element values within the inner or outer boundary and differences between the inner and outer sensing elements.

3 Results and discussion

The study focused on the expanded state of elastomeric balloons (by use of sensing elements) idealized inside multifold lumen structures and we performed a semi quantitative analysis. Given the assumption that the fabricated balloon structure is having compliance that is magnitudes higher compared to the surrounding tissue, it would ideally conform to tissue lumen shape (generally at low pressure) without deforming the tissue.

Table 2: Expansion of thin(1µm) and thick balloon(10µm) within Structure-1. The mentioned length measurements of the Balloon SEs (at full conformal contact with tissue) are tabulated. The differences hold curvature information, and these differences are ~10x larger for the thicker balloon (that is also 10x thicker)

Expansion in 'STR 1'	**SE'nr.'b** [mm] **(B)**	**SE'nr.'a** [mm] **(A)**	**Difference B-A** [µm]
Thin BALLOON: 1[µm]			
nr=1	0.48401	0.48408	-0.07
nr=2	0.48416	0.48380	0.36
nr=3	0.48426	0.48362	0.64
Trend (**SE-1** to **SE-3)**	↑	↓	
Thick BALLOON: 10[µm]			
nr=1	0.48261	0.48335	-0.74
nr=2	0.48425	0.48073	3.52
nr=3	0.48538	0.47895	6.43
Trend (**SE-1** to **SE-3)**	↑↑	↓↓	

It is found that the pressure required for thicker balloon ($10\mu m$) to conform to the shape of tissue geometry with the given dimensions was higher than the thin balloon (1µm). The pressure at which these balloons would conform to the lumen is not relevant to the current study and the analysis was therefore excluded.

The expansion of the two balloons (1µm and 10µm) in structure 1 are tabelled in Table 2 while within structure 2 are tabelled in Table 3. The current length over the outer wall of balloon is found to get higher, the further the tissue lumen is away from the centre of the balloon. It is verified by the stretch value on the Sensing elements being larger from SE-1-a to SE-3-a. In contrast, the exact opposite behaviour occurs in the trend of extension of Sensing Elements on the inner wall of balloon. Here the extension gets larger from SE-3-b to SE-1-b. This trend can also be verified by study conducted by Bhave et. al. [5]. The thicker the balloon used (10x), greater the differences (~10x) were observed within the sensing elements on these structures (verified by inter-elemental differences from SE-1 to SE-3).

Table 3: Expansion of thin(1µm) and thick balloon(10µm) within Structure-2. The mentioned length measurements of the balloon SEs (at full conformal contact with tissue) are tabulated and are larger due to a larger lumen perimeter compared to Structure-1. The differences hold curvature information, and these differences are ~10x larger for the thicker balloon (that is also 10x thicker)

Expansion in 'STR-2'	**SE'nr.'b** [mm] **(B)**	**SE'nr'a** [mm] **(A)**	**Difference B-A** [µm]
Thin BALLOON 1[µm]:			
nr=1	0.55596	0.55633	-0.37
nr=2	0.55617	0.55581	0.36
nr=3	0.55628	0.55552	0.76
Trend (**SE-1** to **SE-3)**	↑	↓	
Thick BALLOON 10[µm]:			
nr=1	0.55383	0.55753	-3.70
nr=2	0.55636	0.55276	3.6
nr=3	0.55772	0.55012	7.6
Trend (**SE-1** to **SE-3)**	↑↑	↓↓	

The expansion of the two balloons within structure 2 are described in Table 3. The extension of balloon (verified through elements) is larger due to a large lumen perimeter visible in structure 2 (Figure 1.c). We see that the lumen region closer to the balloon has a sharper curve in comparison to 'structure 1' (ref Figure 1.b vs 1.c). Correspondingly, we observe larger differences between the outer and inner stretch element (nr=1) in both the balloons expanding within structure 2. We computed the intra-element ratio (IRE) of differences of the SE extension (over inner circumference) of the thin balloon as performed by [5] within 'STR 1' and 'STR 2' (at 10kPa). This intra-element ratio is shown in eq 1.

$$IRE = \frac{\text{Stretched length of } 'SE1a' - \text{of } 'SE2a'}{\text{Stretched length of } 'SE2a' - \text{of } 'SE3a'} \quad (1)$$

Using the thin balloon, this IRE ratio was found to be '1.55' and '1.793' for the 'structure 1' and 'structure 2' respectively; for the thick balloon, these ratios for 'structure 1' and 'structure 2' were '1.47' and '1.806' respectively. This analytical ratio confirms that its values are positively correlated with the lumen sinusoidal shape amplitude (therefore depth). The IRE values also suggest that it may not be necessary that these difference ratios will be larger by choosing a thicker balloon.

To assess the curvature, a simple analogy can be applied: if the inner sensing element has a length lower than that of the corresponding element on the outer wall, then the balloon is curving inside; and curving outside if found to be the opposite. As an example, in Table 2 for 1µm thick balloon, the difference between 'SE1b' and 'SE1a' is (minus) $0.07\mu m$ which indicates that the balloon is curving outwards and can be verified also from the simulation. Both the balloons in both the structures reveal that the balloon at SE1 pair is curved outside while the other two regions are curved inside. The thicker the balloon used(10x), greater the differences(~10x) that were observed within the sensing elements these structures (verified by length differences within element on outer wall and inner wall).

4 Conclusion

This initial study provides logical analysis obtaining the curvature of tissue (lumen profile) and depth information through sensing elements on a sensor-actuator setup. A simple inner to outer Sensing Element difference may hold curvature information and help in recreating the lumen profile and needs to be further validated for different situations.

Sensitivity of the system must be high to capture the differences. It may be ideal to manufacture thicker balloons that may have a very high compliance in comparison to the surrounding tissue (at least for the initial conformal contact) to obtain clear measurable differences (that are usually less affected by signal-noise ratio).

Based on the important points from the current study, it is intended to further the simulations with 3D setup and anisotropic characterization of vessels to obtain more realistic measurements and try to obtain simplified analytical solutions for tissue property identification.

Author Statement

This research was partly supported by the German Federal Ministry of Research and Education (BMBF) under grant no. 13FH5I05IA (CoHMed/Digitalization in the OR) and under grant no. 2522FSB903-PerFluid (ERA PerMed).

References

[1] Sittkus B, Zhu R, Mescheder U. Flexible piezoresistive PDMS metal-thin-film sensor-concept for stiffness evaluation of soft tissues. In: 2019 IEEE International Conference 7/2019: 1–3.

[2] Cunnane EM, Davis NF, Cunnane CV, et al. Mechanical, compositional and morphological characterisation of the human male urethra for the development of a biomimetic tissue engineered urethral scaffold. Biomaterials 2021; 269: 120651.

[3] E. Martins F, Simoes de Oliveira P, M. Martins N. Historical Perspective and Innovations in Penile Urethroplasty. In: Pang R, editor. Lower Urinary Tract Dysfunction - From Evidence to Clinical Practice: IntechOpen; 2020.

[4] Bhave A, Möller K. Comparison of a histology based multi layer artery model to its simplified axisymmetric model. Current Directions in Biomedical Engineering 2021; 7: 590–593.

[5] Bhave A, Rupitsch SJ, Moller K. Simulation study of inflation of a high compliant balloon inside idealized non-linear tissue geometry. Current Directions in Biomedical Engineering 2022; 8: 672–675.

[6] Bhave A, Sittkus B, Rupitsch SJ, Knut Moeller, editors. Evaluation of high compliant elastomer balloons for the identification of artery biomechanics: Proceedings on Automation in Medical Engineering 2023.

[7] Bernardi L, Hopf R, Ferrari A, Ehret AE, Mazza E. On the large strain deformation behavior of silicone-based elastomers for biomedical applications. Polymer Testing 2017; 58: 189–198.